INTERNATIONAL ATOMIC ENERGY AGENCY
UNITED NATIONS EDUCATIONAL, SCIENTIFIC AND CULTURAL ORGANIZATION

INTERNATIONAL CENTRE FOR THEORETICAL PHYSICS
34100 TRIESTE (ITALY) - P.O.B. 586 - MIRAMARE - STRADA COSTIERA 11 - TELEPHONES: 224281/2/3/4/5/6
CABLE: CENTRATOM - TELEX 46392 ICTP

SMR-30/ 29

WINTER COLLEGE ON ATOMIC AND MOLECULAR PHYSICS

26 January - 18 March 1977

ULTRAHIGH RESOLUTION SATURATED ABSORPTION SPECTROSCOPY

(Taken from "Laser Spectroscopy")

C. BORDÈ and J.L. Hall

ULTRAHIGH RESOLUTION SATURATED ABSORPTION SPECTROSCOPY*

Ch. Bordé† and J. L. Hall‡

Joint Institute for Laboratory Astrophysics

National Bureau of Standards and University of Colorado

Boulder, Colorado 80302

In this paper we report our progress in the search for super narrow lines, our present state of the art in the line shrinking business and what looks like the way towards still higher resolution based on our current knowledge of the broadening mechanisms.

It is conventional wisdom that the natural linewidth is the only fundamental limit to ultrahigh resolution in saturated absorption spectroscopy. Still it appeared that an actual experimental attempt to achieve such ultrahigh resolution might teach us about some other realistic limitations.

The test molecule we chose was, of course, methane. Its narrow natural linewidth (<100 Hz)[1] and easy wavelength coincidence[2] with the He-Ne laser at 3.39 μm have been noted before. The high resolution potential has motivated development of several appropriate laser devices for such a study. Actually methane may not be the most favorable case for obtaining very narrow lines because it is a light molecule, but it has remarkable features:

(1) It shows a well resolved magnetic hyperfine structure,[3] providing an unambiguous natural frequency scale.

(2) Precisely because it is a light molecule, it helps the study and the understanding of all the broadening factors

†Supported by CNRS; also NATO Fellow, 1973.

‡Staff member, National Bureau of Standards, Boulder, Colorado.

that decrease with increasing mass--these are the transit-time broadening, the second-order Doppler shift and broadening, and mainly the recoil structure.

(3) A careful study of the CH_4 lines at 3.39 μm is interesting in connection with their possible applications as a wavelength or frequency standard.[4]

To discuss the linewidth problem in a detailed way, a good starting point may be the two equations that the molecules must satisfy simultaneously to be able to interact with two waves having the same frequency ω_L but opposite wave vectors $\pm\underline{k}_L$:

$$\begin{cases} \omega_L = \omega_0 + \underline{k}_L \cdot \underline{v} \\ \omega_L = \omega_0 - \underline{k}_L \cdot \underline{v} \ . \end{cases} \qquad (1)$$

For resonance, the laser frequency ω_L should be equal to the resonant frequency of the molecule ω_0 shifted by the first-order Doppler effect. The well-known solution to this problem is $\omega_L = \omega_0$ and $\underline{k}_L \cdot \underline{v} = 0$. In fact each one of these quantities contains some uncertainty which ultimately appears as a broadening mechanism for the saturation resonance.

For ω_L this is the laser spectral width. The basic requirement for high resolution spectroscopy is to have a source whose frequency stability is appreciably better than the desired resolution.

The molecular absorption frequency ω_0 is affected by the finite natural lifetime. This is the only fundamental limit in saturated absorption spectroscopy, for the methane lines we estimate it to be less than 100 Hz. ω_0 is also affected by the collisions and by the Zeeman effect due to the earth's magnetic field. These two broadening causes can be reduced to a negligible value. Internal interactions may also split ω_0 into several resonant frequencies which, if unresolved, will give an extra inhomogeneous character to the line. For example, this was the case before we resolved the methane hyperfine structure.

The last term describes the first-order Doppler broadening. To obtain sub-Doppler resolution in conventional spectroscopy, the experimenter may constrain the function $\underline{k} \cdot \underline{v}$ using molecular beam techniques. In the present saturated absorption experiments we rely on the light both to select the $\underline{v}$ and to probe the selected molecules.

If there is a distribution in the spatial frequencies, that is, if the waves are misaligned or are not perfectly plane, there is going to be a residual first-order Doppler broadening in saturated absorption spectroscopy.

Thus the success of laser saturated spectroscopy is not only due to the laser's very narrow spectral distribution of ω_L but also to its ability to produce a wave with a very narrow distribution of k_x k_y k_z. How well one can do in saturated absorption spectroscopy will clearly depend on how well one can produce a monochromatic wave and on how well one can produce a plane wave.

To achieve the necessary frequency stability it is absolutely essential to electronically control the laser frequency. The most powerful concept known to us is called frequency offset locking[5,6] whereby one acquires good frequency stability with one laser device and transfers the stability to the laser used to explore the molecular resonances. Our present apparatus is shown in Fig. 1. Its reference laser has a 5-power internal telescope which reduces the reference methane saturation peak width to 50 kHz HWHM.

FREQUENCY OFFSET-LOCKED LASER SPECTROMETER

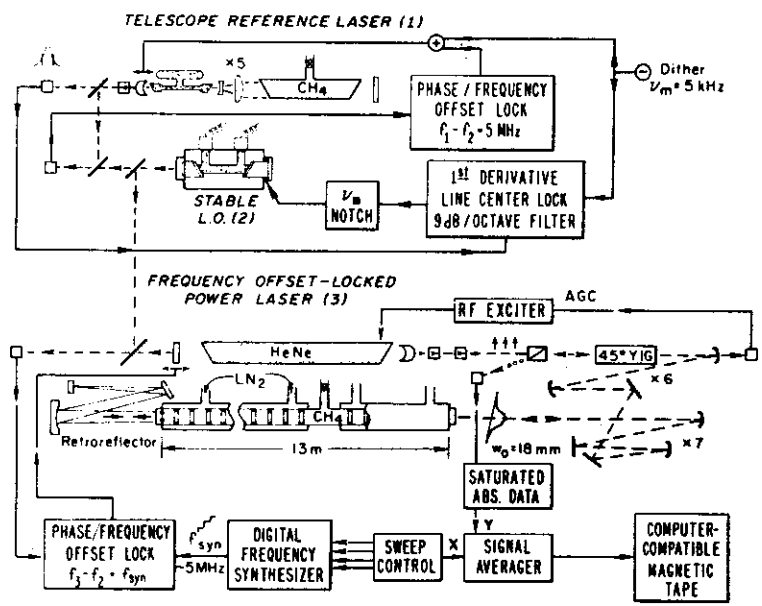

Figure 1

A "solid ingot" local oscillator laser, phase locked 5 MHz red from the methane line, provides the (offset) output frequency of the reference system. Finally, the power laser is phase locked relative to the stable local oscillator using a tunable frequency offset to scan the studied line. To achieve this controlled tuning, the beat frequency between the last two lasers can be varied by digital request to a frequency synthesizer which is in this second heterodyne offset loop. Thus one has both frequency stepping capability and very high frequency stability, along with a natural and stable correspondence being made between offset frequency and channel number of the signal averager.

The power laser's frequency stability is approximately $3 \times 10^{-13}\tau^{-1/2}$ for an averaging time τ in the range $10^{-2} < \tau < 10^{2}$ sec. At shorter times the noise is characterized by a linewidth which we estimate to be about 500 Hz. At longer times the frequency stability fails to improve beyond 3×10^{-14} (3Hz rms) for $10^{2} < \tau < 10^{4}$ sec, due to changes in the systematic errors which limit the present reproducibility to about ± 300 Hz. We think those offsets are partly due to the intensity-dependent shifts to be discussed later.

Let us come now to the k distribution. We want it as narrow as possible. Because of diffraction, to obtain a narrow angular distribution we want the beam diameter as big as possible. An appropriate Fourier transformation relates the two corresponding widths. We may write

$$\Delta k_{\perp}\ \Delta x \simeq 1 \quad ,$$

where Δx will be taken as the beam waist radius. Thus we calculate, using Eq. (1), a residual Doppler broadening due to the transverse velocity

$$\Delta\omega = \underline{\Delta k}_{\perp} \cdot \underline{v} \simeq \frac{1}{w_0} v \quad \text{diffraction} \ .$$

We can equivalently understand this broadening as due to the finite transit time of the molecule flying across the beam:

$$\Delta\omega \simeq \frac{1}{\Delta t} \simeq \frac{v}{w_0} \quad \text{transit time} \ .$$

So with either approach, the linewidth times the beam radius is expected to be a constant having the dimensions of a velocity: we write

$$\Delta\nu_{HWHM} \times w_0 = k_v \ .$$

This relation is illustrated on Fig. 2. For methane we find

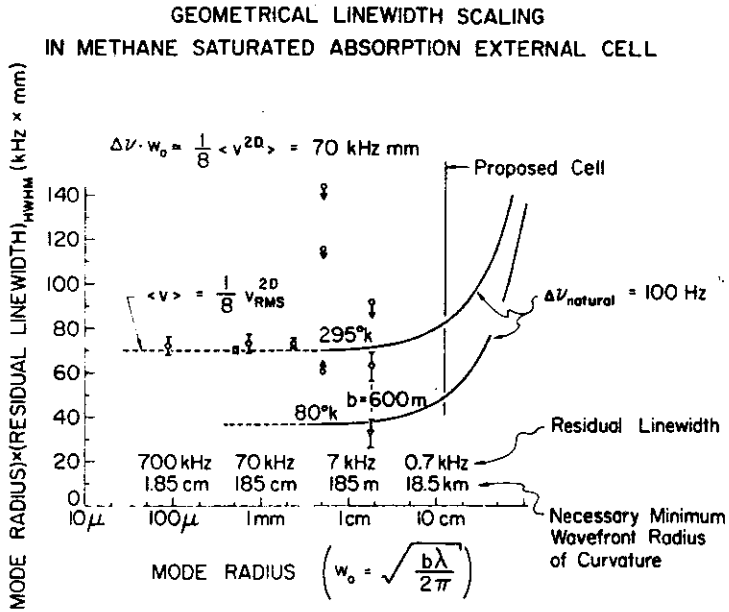

Figure 2

$k_v \simeq 1/8(2kT/M)^{1/2}$ which is 70 kHz mm at room temperature. Liquid nitrogen narrows the lines by about a factor of two. In our last experiment two successive reflective telescopes were used to expand the beam by a factor of 42. However, due to imperfect cell straightness, the effective beam had an 18 mm mode radius, which gives us about 4 kHz contribution to the linewidth at room temperature.

In the pursuit of narrow saturation resonances we must also beware of wave front deviations from the ideal beam considered above: Of course there are many ways that laser beams can have more angular content than is imposed by their fundamental diffraction limit. One can easily observe such effects as back surface reflections in mirrors, imaging aberrations, beam deformation by the air path, and non-ideal output mode structure of the laser. Similarly the retroreflected probe must be parallel, colinear and have matched (planar) wavefronts. To achieve this alignment condition, we use a "cat's eye" retroreflector as illustrated in Fig. 1. The 100 μW return beam is steered to the detector by polarization optics: a Faraday rotator (45° YIG) and a Rochon prism comprise this optical directional coupler. The cell has a 5 cm diameter, is 13 m long and filled with CH_4 at pressures around 100 μTorr or less.

The part of the CH_4 spectrum that one can cover with the He-Ne laser at 3.39 μm is represented in Fig. 3. This is a conventional spectrum of the Coriolis fine structure P(7) of ν_3.[7]

The ν_3 vibration has the carbon atom vibrating relative to the tetrahedral frame of hydrogen. Tetrahedral symmetry is sufficiently high that the three perpendicular vibration modes of the carbon against the tetrahedral frame must be degenerate. Thus, in the excited vibrational state a linear combination can be formed in which a circulation is evident. There is a resulting angular momentum $\underline{L}$ that is coupled to the rotational angular momentum of the frame $\underline{R}$ to give the total angular momentum $\underline{J}$. Some of the degeneracy within a given J manifold is lifted in the ground state by centrifugal distortion, but this term is small compared with the Coriolis perturbation that appears in the excited state. These effects result in six components for the transition of interest, P(7). The laser emission is centered in close coincidence to the F component at 2947.912 cm^{-1}. This is the line that we have first studied without any special trick.[6] With permanent magnets Zeeman shifting the laser emission, we have also studied the E component.[8]

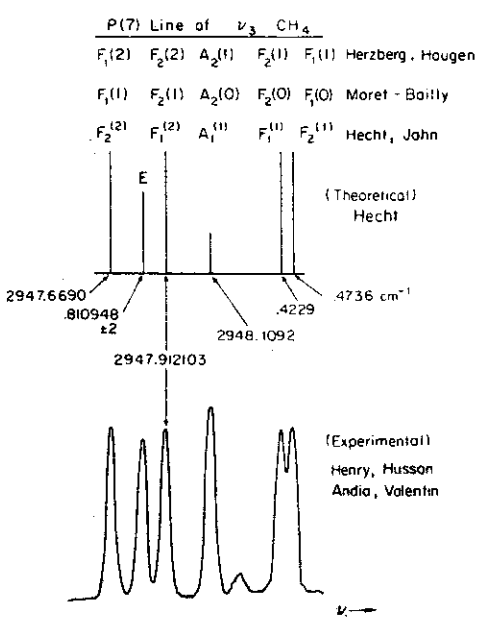

Figure 3

With an electromagnet we observed the A component, and with superconducting solenoids one probably could cover all six Coriolis components. In Fig. 3 we also show the most popular notations for these Coriolis components.[9,10] The notation adopted here is that of Herzberg[11] and Hougen.[12] The important thing is that the F components correspond to levels having a total nuclear spin I = 1 for the four hydrogens, whereas I = 0 for the E line.

Figure 4 shows a typical derivative spectrum for the $F_2^{(2)}$ component. Whereas the spectrum for the E line is a single line, this spectrum exhibits three strong lines. On the low frequency side there is a weaker and broader line, and on the 15 times magnified picture two additional very weak lines are visible. The intensities are in the approximate ratios $1:(1/20):(1/20)^2$.

As noted above the two levels of the observed $F_2^{(2)}$ transition have a total nuclear spin I = 1. Thus, there are three combinations to be formed coupling $\underline{I}$ and $\underline{J}$ to form $\underline{F} = \underline{I} + \underline{J}$. Corresponding to J = 7 in the ground state, the F levels will be 6, 7, and 8 and corresponding to J = 6 in the excited state the F levels will be 5, 6, and 7.

The degeneracy of these levels is removed by magnetic interaction terms in the Hamiltonian. For the ground state these are: a scalar and a tensor spin-rotation interaction and a spin-spin interaction between the protons; for the excited state one expects also a spin-vibration interaction with both scalar and tensor parts.[13]

From the theory of the relative intensities in a multiplet we expect three main diagonal lines for which $\Delta F = \Delta J = -1$, with intensities which increase with F. So we identify the + 9.7 kHz line as the 8↔7 transition, the central line at -1.7 kHz as 7↔6 and the low -12.8 kHz one as 6↔5. Besides these lines one expects two much weaker satellite lines with $\Delta F = 0$ that we identify with the two weak low frequency lines.

In addition to these usual components, saturated absorption spectroscopy provides a new resonance each time two transitions share a common level. This is a distinctive feature of saturated absorption spectroscopy. These three level resonances are called "Doppler-generated level crossings." They occur half way between the two usual transitions and have an intensity proportional to the geometrical mean of the two parent lines. We have four of these represented in Fig. 4. To reproduce the spectrum near -38 kHz with these crossings we have to assume that the -72.0 kHz peak is the 6↔6 and that the -91.2 kHz peak is the 7↔7. The transitions indicated in the energy level diagram are arranged in the same order as the spectral lines, with higher absolute frequency to the right.

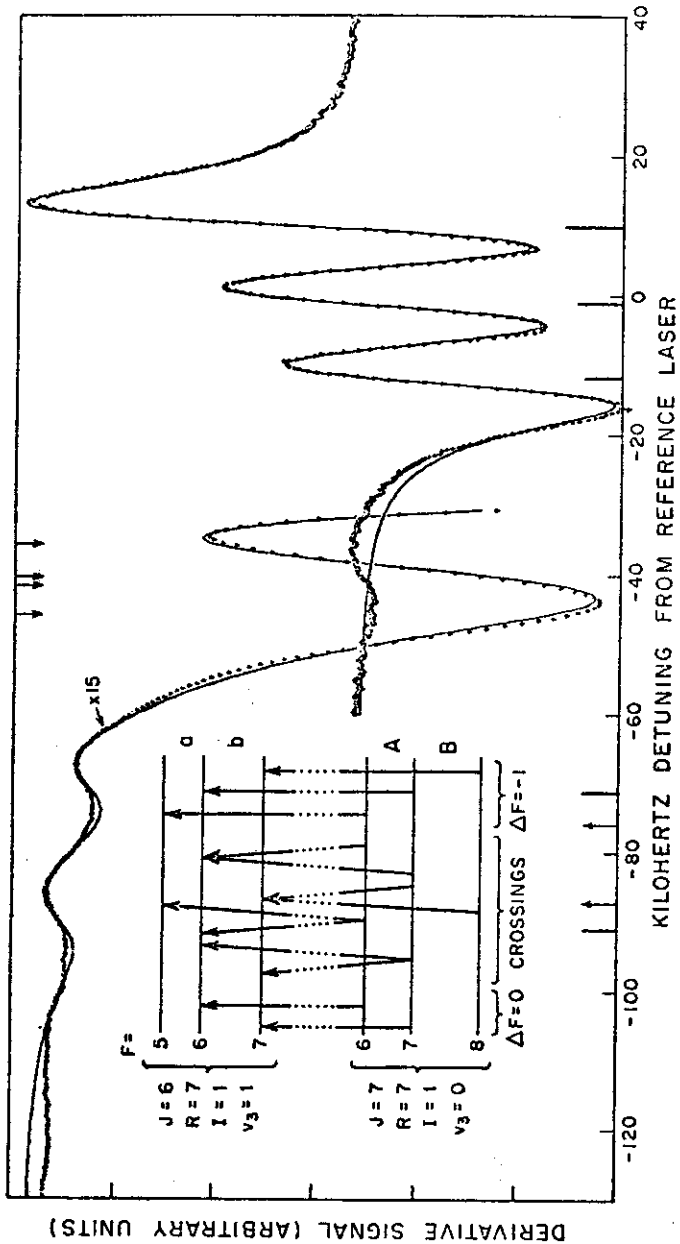

Figure 4. Composite saturated absorption hyperfine spectrum: experimental data ×, least-squares fit ——. T = 77°K. Main triplet: methane pressure 70 μTorr, modulation 2 kHz peak-to-peak at 600 Hz. Fitted Lorentz width = 5.8 kHz HWHM. Low frequency spectrum taken at lower resolution, ~9.8 kHz HWHM. The unobserved ΔF = +1 line and its crossings are not illustrated on the energy level diagram.

With this interpretation we find the values of the energy intervals given in Table I. The experimental values have an uncertainty of ± 1.5 kHz arising primarily from measurement of the weak lines. These experimental values are to be compared with those recently calculated by Jon Hougen[13,14] for the ground state, using the constants derived from the magnetic resonance experiments by Yi, Ozier and Ramsey.[15] The agreement is just within the uncertainties of both experiments. As pointed out by Dr. Hougen,[14] it is not obvious that the agreement should be any better: the hyperfine coupling constant may be J dependent because of the centrifugal distortion of the molecule. This experiment also demonstrates that one can have access to knowledge of the hyperfine splittings of a vibrationally excited state.

The least-squares fit of the main components in the spectrum of Fig. 4 gave us a linewidth HWHM equal to 5.8 kHz. Recently, this was a typical result for a room temperature spectrum. To account for the linewidth, we must consider effects omitted in Eqs. (1) which are no longer negligible. These are the second-order Doppler shift and the recoil effect. Both come out of a proper relativistic energy and momentum balance. In the laboratory frame we may write

$$\hbar\omega = \sqrt{P_b^2c^2 + (Mc^2+E_b)^2} - \sqrt{P_a^2c^2 + (Mc^2+E_a)^2} \qquad (2)$$

$$\hbar\underline{k} = \underline{P}_b - \underline{P}_a \quad .$$

Here let the "b" subscript refer to the upper level. An expansion to the order $1/c^2$ yields shifted absorption and emission resonance frequencies

$$\omega_{absorption} = \omega_o + \underline{k}\cdot\underline{v}_a - \omega_o \frac{v^2}{2c^2} + \frac{\hbar\omega^2}{2Mc^2}$$
$$\omega_{emission} = \omega_o + \underline{k}\cdot\underline{v}_b - \omega_o \frac{v^2}{2c^2} - \frac{\hbar\omega^2}{2Mc^2} \quad . \qquad (3)$$

Table I. Energy level differences illustrated in Fig. 4.

Level	Interval	Experiment*	Calculation†	pure Ca $\underline{I}\cdot\underline{J}$‡
$v_3 = 1$	a	59.2 kHz		62.4 kHz
	b	89.5		72.8
$v_3 = 0$	A	70.3	68.4 kHz	72.8
	B	100.9	99.7	83.2

*Ref. 3 †Ref. 14 ‡Calculated using Ca = 10.4 kHz (Ref. 15)

The v^2 term leads to a second-order Doppler shift of ≈ 0.5 Hz/°C for methane.[16] Since we deal with a thermal distribution of velocities, this shift will also be accompanied by a broadening effect. The last term is the recoil frequency shift, which leads to an absorption/emission frequency difference $\hbar\omega^2/Mc^2 = 2.16$ kHz[17] for the CH_4 line of interest. We can rewrite Eqs. (1) expressing the saturated absorption resonance condition,

$$\text{lower state resonance} \begin{cases} \omega_L = \omega_o + \underline{k}\cdot\underline{v}_a - \omega_o \dfrac{v^2}{2c^2} + \dfrac{\hbar\omega^2}{2Mc^2} \\ \omega_L = \omega_o - \underline{k}\cdot\underline{v}_a - \omega_o \dfrac{v^2}{2c^2} + \dfrac{\hbar\omega^2}{2Mc^2} \end{cases}$$

$$\text{upper state resonance} \begin{cases} \omega_L' = \omega_o + \underline{k}\cdot\underline{v}_b - \omega_o \dfrac{v^2}{2c^2} - \dfrac{\hbar\omega^2}{2Mc^2} \\ \omega_L' = \omega_o - \underline{k}\cdot\underline{v}_b - \omega_o \dfrac{v^2}{2c^2} - \dfrac{\hbar\omega^2}{2Mc^2} \end{cases} . \qquad (4)$$

There are two saturation resonance peaks now, for $\underline{k}\cdot\underline{v}_a = 0$ and $\underline{k}\cdot\underline{v}_b = 0$ with the corresponding resonance frequencies

$$\omega_L = \omega_o - \omega_o \frac{v^2}{2c^2} + \frac{\hbar\omega^2}{2Mc^2}$$

and

$$\omega_L' = \omega_o - \omega_o \frac{v^2}{2c^2} - \frac{\hbar\omega^2}{2Mc^2} . \qquad (5)$$

This double peak structure has been previously predicted by Kol'chenko, Rautian, and Sokolovskii.[18]

To the two sets of Eqs. (4), there are two corresponding sets of lines on the ω vs. v plot of Fig. 5. The upper pair of lines corresponds to the ground state. From the figure one can see that the population peaks created in the excited state cross each other for a laser frequency lower than that for which the holes cross each other. Note that for a three-level resonance only one level is involved--that is the common level. So there we expect only a red or a blue component depending on whether we have a common upper or lower level.

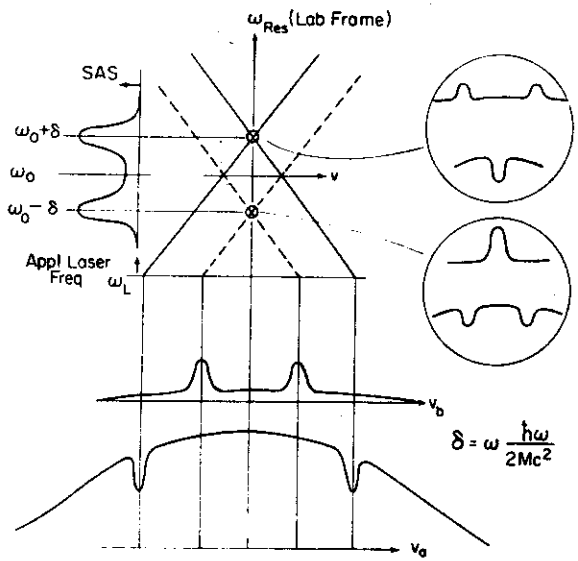

RECOIL – INDUCED DOUBLET

Figure 5

The recoil structure has not yet been observed in saturated absorption spectroscopy, but our highest resolution line shapes are consistent with the existence of the doublet. Figure 6 illustrates the best resolution we have obtained by cooling the cell to liquid nitrogen temperature. In view of the time, expense and labor that will precede experimental data of adequate resolution to display the recoil doublet, perhaps we may be forgiven a brief attempt to "hyper-analyze" the existing data. The least-squares fit in Fig. 6 gave a 4.14 kHz linewidth but the fit is not very good--the experimental data are straighter at line center than either a Lorentz or a Gaussian. The line wings are Lorentzian, but decrease faster than the Lorentzian which fits the peak-to-peak separations. These differences are more apparent if one imposes a fit at the derivative peaks rather than allowing the unweighted least-squares fit. Modulation broadening[19] can give a somewhat similar effect, but accounts for only 1/15 of the present effect. The line shape in the free-flight regime has been shown to be accurately Lorentzian.[20]

Thus it was interesting to try to fit the spectrum of Fig. 6 with each component being a (recoil) doublet. A common splitting and height ratio were adopted as additional fitting parameters in the least-squares fitting program. Miraculously the program

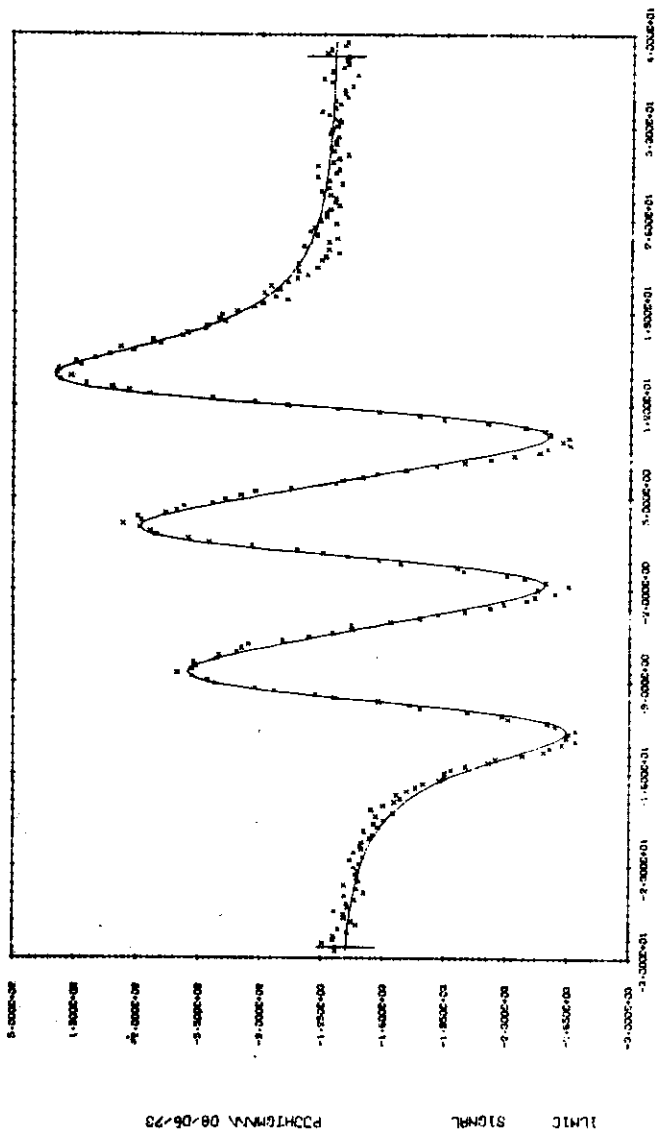

Figure 6. Lorentz least-squares fit to highest resolution data.

converged, giving a 55/45 height ratio and a splitting of (2.22±.04) kHz! Starting the initial height ratio at 10:1 or the splitting at 1/2 or 2 times the preceding value gave convergence to the same final splitting. The doublet fit reduced the variance of the residuals from 2.9 times the expected white noise variance to only 1.26 times this value. Figure 7 shows the doublet fit to the data of Fig. 6.

Two other high resolution data sets were available. Fits to both were also significantly improved, and converged to doublet splittings of (2.03 $\pm$ .05)kHz and (2.20 $\pm$ .02)kHz with height ratios of 60/40 and 51/49. The low frequency peak intensity is favored above 50/50 by 3, 5 and 1 standard deviations in the three cases. All these quoted errors are on a "one standard deviation" basis and contain no allowance for systematic effects. We conclude that our best data like a doublet representation but that an increment in resolution will be necessary to remove all doubts.

To make a comparison with conventional spectroscopy, the present linewidth is 3 kHz, which corresponds to 10^{-7} wave numbers. We have thus demonstrated at 3000 wave numbers a resolving power of 2.4×10^{10}, where we understand zero second derivative as the resolution condition.

Since we have achieved the diameter-scaling linewidth contribution (1.9 kHz) at liquid nitrogen temperature, it is interesting to estimate the other linewidth contributions:

1)	natural linewidth	<100 Hz
2)	second-order Doppler broadening	≈100 Hz
3)	pressure broadening at 30 μTorr	≈300 Hz
4)	residual earth's field Zeeman broadening	≈100 Hz
5)	saturation broadening	≤200 Hz
6)	modulation broadening	≈300 Hz
7)	laser spectral width	≈500 Hz

Most of these broadening contributions are resistant to further important reductions, but it still appears that another major improvement can be obtained by increasing the cell aperture. A cell of 38 cm aperture, 14 m length using internal reflective optics is being prepared. The potential increment in resolution should make possible a careful study of the line shapes of the two recoil peaks. It is interesting that if the two-state lifetimes are not equal, the peak heights of the doublet will be different. A dependence of the relative strengths of the two lines on experimental param-

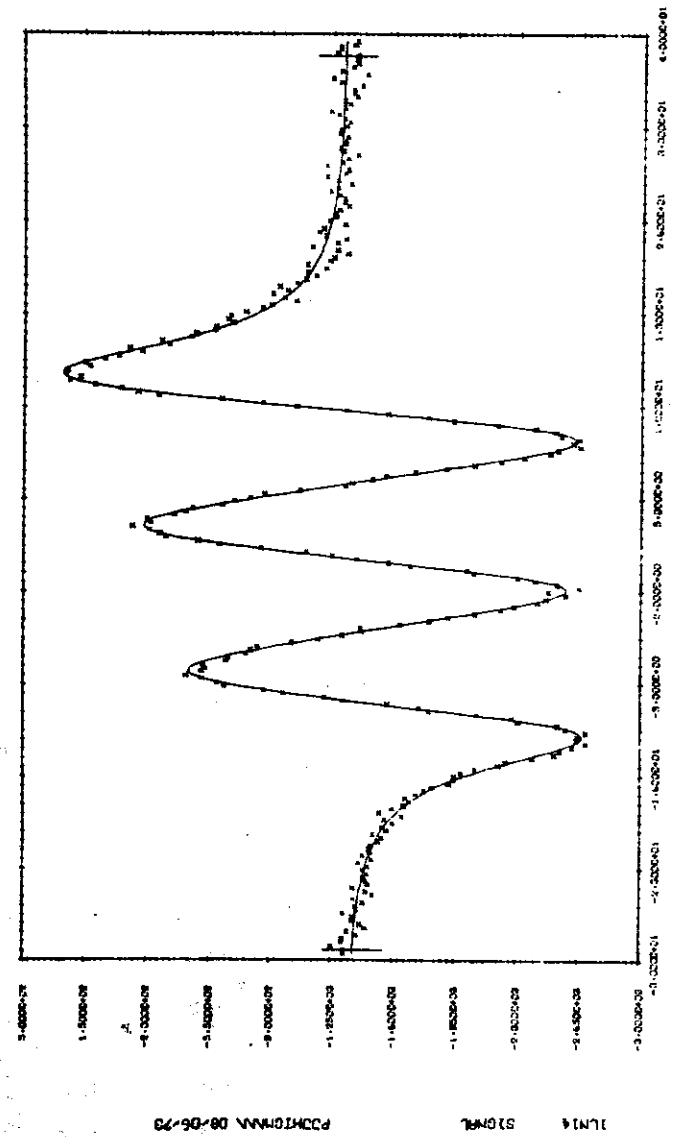

Figure 7. Lorentz doublets fit to data of Fig. 6.

eters will certainly affect the frequency reproducibility achievable with saturated absorption frequency standards. At low resolution such differential shifts may be avoided by choice of a regime in which both levels are dominated by the same relaxation mechanisms.

Another important example of the effect of unresolved structure on the frequency reproducibility of a stabilized laser is of course also provided by the presence of hyperfine structure in methane. This effect is illustrated in Fig. 8 where we have a synthetic derivative of the peak versus frequency for different saturation parameters. A linewidth of 50 kc was assumed corresponding to our reference telescope laser. Since the intensity of the different components is a non-linear function of the optical field, the apparent zero crossing of the derivative of the unresolved line is shifted towards low frequencies as the saturation increases.[21] This means an intensity-dependent red shift of a laser stabilized at the apparent center of this line. The consequence is that long term stability using the F component will require careful stabilization of the intensity, or sufficient resolution to separate the structure. Alternatively we can use the E Coriolis component which is free of this type of hyperfine structure.

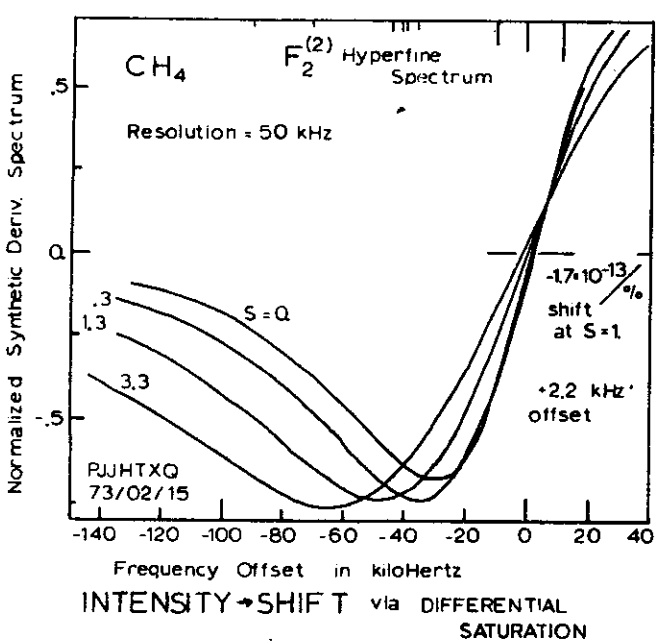

Figure 8

Since the reference laser at present does not have such an intensity stabilizer, we were not able to make a reliable measurement of the second-order Doppler shift upon cooling the long cell from room temperature to 77°K. In the absence of a proper theory which relates the signal contribution to the molecular transverse velocity, it is not obvious what mean velocity to use in the second-order Doppler term of Eq. (5). In particular, in the transit-limited domain at low pressures, we may expect the effective transverse velocity to increase with the laser power.

In this paper we have discussed the several factors which limit our present spectral resolution to 2.4×10^{10}. Some effects such as the methane hyperfine structure have been elucidated; the hyperfine energy splittings of an excited state have been obtained. With the higher resolution expected in the near future, it should be interesting to further investigate the recoil structure as well as the Doppler-generated level-crossing resonances. Ramsey double excitation methods may prove an attractive alternative to simple diameter magnification for exceptionally long-lived molecules. Perhaps storage techniques for ions--eventually neutrals--can be used to obtain dramatically lengthened interaction times.

Acknowledgments

The authors wish to thank several of their colleagues for valuable discussions. Drs. A. C. Gallagher and P. L. Bender have sharpened our understanding of the free-flight regime.

We thank Dr. Judah Levine for providing some numerical filters and for assistance with other topics in applied computerology.

Especially we are indebted to Chela Kunasz for expert and cheerful help with the least-squares fitting program. The glimpse inside the linewidth would not have been possible without her skillful and enthusiastic help.

References

1. R. B. Armstrong and H. L. Welsh, quoted by J. T. Yardley and C. B. Moore, J. Chem. Phys. 49, 1111 (1968).

2. H. J. Gerritsen and M. E. Heller, Appl. Opt. Suppl. #2, 73 (1965). See also K. Sakurai and K. Shimoda, Japan J. Appl. Phys. 5, 744 (1966).

3. J. L. Hall and Ch. Bordé, Phys. Rev. Letters 30, 1101 (1973).

4. In their June, 1973, Paris meeting, the Comité Consultatif pour la Définition du Mètre recommended a wavelength value for the methane P(7) F component, $\lambda = 3392231.4 \times 10^{-12}$ m. They also recommended a value for a certain iodine transition at .633 μm and for the speed of light, c = 299,792,458 m/sec. The assigned fractional uncertainties of these quantities is $\pm 4 \times 10^{-9}$.

5. J. L. Hall, IEEE J. Quant. Electron. QE4, 638 (1968).

6. R. L. Barger and J. L. Hall, Phys. Rev. Letters 22, 4 (1969).

7. Spectrum from L. Henry, N. Husson, R. Andia, and A. Valentin, J. Mol. Spectry. 36, 511 (1970).

8. J. A. Magyar and J. L. Hall, Bull. Am. Phys. Soc. 17, 67 (1972); and J. A. Magyar, to be published.

9. J. Moret-Bailly, J. Mol. Spectry 15, 344 (1965).

10. K. T. Hecht, J. Mol. Spectry. 5, 355 and 390 (1960).

11. G. Herzberg, Electronic Spectra of Polyatomic Molecules (Van Nostrand, Princeton, N.J., 1967), p. 102.

12. J. T. Hougen, J. Chem. Phys. 39, 358 (1963).

13. J. T. Hougen, private communication.

14. J. T. Hougen, 28th Symposium on Molecular Structure and Spectroscopy, The Ohio State University, Columbus, Ohio, June, 1973; and to be published.

15. P. N. Yi, I. Ozier, and N. F. Ramsey, J. Chem. Phys. 55, 5215 (1971).

16. S. N. Bagaev and V. P. Chebotayev, ZhETF Pis. Red. 16, 614 (1972) [JETP Lett. 16, 433 (1972)].

17. The recoil splitting quoted in Ref. 3, 2.4 kHz, is unfortunately in error. The proper splitting is 2.44×10^{-11} fractional shift, which is 2.16 kHz.

18. A. P. Kol'chenko, S. G. Rautian, and R. I. Sokolovskii, ZhETF 55, 1864 (1968) [Sov. Phys. - JETP 28, 986 (1969)].

19. R. L. Smith, J. Opt. Soc. Am. 61, 1015 (1971); also H. Wahlquist, J. Chem. Phys. 35, 1708 (1961).

20. J. L. Hall, in Atomic Physics 3 edited by S. J. Smith and G. K. Walters (Plenum, New York, 1973), pp. 615-646.

21. J. L. Hall and Ch. Bordé, Proceedings of the 27th Annual Symposium on Frequency Control, Cherry Hill, N. J. (June 1973).